Open Access

Iraqi Journal of Industrial Research (IJOIR)

Journal homepage: http://ijoir.gov.iq

GIS-Based Assessment of Air Pollutants in Erbil, Kurdistan-Iraq through Seasonal and Monthly Variations in Air Quality

[1]Muzhda Qasim Qader*, [2]Siraj Muhammed Abdulla Goran

[1]Department of Public Health, College of Health Sciences, Hawler Medical University, Kurdistan Region, Iraq

[2]Environmental Science and Health Department, Salahaddin University-Erbil, Iraq

Article information

Article history:
Received: May, 29, 2025
Accepted: August, 04, 2025
Available online: December, 14, 2025

Keywords:
Air quality,
Air pollutants,
GIS-based analysis,
Environmental monitoring,
Public health

Corresponding Author:
Muzhda Qasim Qader
muzhda.qadir@hmu.edu.krd

DOI:
https://doi.org/10.53523/ijoirVol12I2ID573

Abstract

Air pollution in Erbil, Kurdistan Region of Iraq, has increased significantly in recent years, due to rapid urbanization, increased vehicular emissions, industrial activities, and the use of low-quality fuels. This study assessed the monthly variation of key air pollutants in Erbil, Iraq, over a 12-month period, focusing on carbon monoxide (CO), formaldehyde (HCHO), methane (CH_4), nitrogen dioxide (NO_2), ozone (O_3), sulfur dioxide (SO_2), and ultraviolet (UV) radiation. The data analysis revealed that CO concentrations ranged from 5.90 ppm in October to 7.42 ppm in June, with a mean of 6.66 ppm. Formaldehyde levels varied between 0.0124 ppm and 0.0382 ppm, peaked in summer months, while methane showed minimal variation around 4.67 ppm. Nitrogen dioxide ranged from 0.0512 ppm to 0.1004 ppm, with higher levels observed in warmer months. Ozone concentrations fluctuated between 0.2997 ppm and 0.3684 ppm, exceeding WHO guidelines throughout the year. Sulfur dioxide showed significant seasonal variability, rose to 0.0232 ppm in December. The UV index varied markedly, with a maximum of 16.76 in January and a minimum of 6.35 in June. Regression analysis revealed significant negative trends for CO and UV, while HCHO, CH_4, and SO_2 revealed increasing trends over time. Air Quality Index (AQI) values indicated consistently high levels of O_3 and NO_2 reached hazardous levels. Correlation and principal component analyses identified CO and NO_2 as the primary contributors to air pollution. The findings demonstrated notable seasonal and spatial variability, with pollutant concentrations frequently exceeding WHO limits, highlighting the urgent need for effective air quality management in Erbil.

1. Introduction

Air pollution is a major environmental and public health concern worldwide. Erbil, the capital of the Kurdistan Region in Iraq, has experienced rapid urbanization and significant industrial expansion, factors that are likely to intensify current air quality challenges. Air pollution consists of a mixture of gases, liquids, and solids that, when present in sufficient quantities, adversely impact human health and the environment [1, 2]. Air quality directly

impacts the well-being of people and the economy [3]. Major primary air pollutants include gaseous pollutants such as SO_2, NO_2, and CO. Secondary pollutants include ozone (O_3), sulfuric acid (H_2SO_4) (acid rain), ammonium nitrate (NH_4NO_3) among others, which develop in the atmospheric system from primary pollutants [4]. Over 40% of Iraq's land is desert, and there are typically 122 sand and dust storms per year. The wind pattern, climatic condition, and characteristics of terrain also contribute to the genesis of an intense dust storm, thereby leading air pollution [5, 6]. Currently, in the post-war longevity, industrial development is taking place and causing air pollution [7]. The Kurdistan Region of Iraq (KRI) has experienced environmental degradation, including a 51% reduction in green fields due to drought and urban population growth from 4.66 million in 2013 to 6.56 million in 2023 [8]. Al-Salman and Taghiebadi in 2021 [9], revealed that SO_2, NO_2, and CO_2 are the major air pollutants in Iraq. Sulfur compound levels have reached dangerous thresholds, posing significant risks to human health [10]. The increasing concentration of harmful gases in the atmosphere has led to a rise in serious health issues, including respiratory and carcinogenic diseases. Numerous studies have demonstrated that the rising number of carcinogenic diseases, mostly of which are related to air pollution, has led to a public health crisis in Iraq and Erbil-Kurdistan [11-13]. The Air Quality Index (AQI) is a standardized framework used to convert ambient concentrations of key air pollutants into a single numerical value that reflects their potential health impact. It typically ranges from 0 to 500, with higher values indicating more severe air quality conditions, as defined by the United States Environmental Protection Agency (US EPA) [14, 15]. Each range is associated with specific health concern levels, enabling clearer communication of air pollution risks to the public and decision-makers. In parallel, the World Health Organization (WHO) Risk Percentage is utilized to quantify the extent to which measured pollutant levels exceed internationally recommended thresholds. This index provides a population-based perspective on exposure risk, serving as an important metric for evaluating public health implications in regions experiencing elevated pollutant concentrations [16, 17]. The lack of updated, city-specific data on air pollutants in Erbil hinders effective policy-making and public health interventions. This study utilizes GIS technology to map and analyze the spatial distribution and quantify concentrations of NO_2, SO_2, CH_4, O_3, CO, HCHO, and UV radiation in the Erbil region of Kurdistan, Iraq.

2. Material and Methods

2.1. Local Geography of Erbil-Kurdistan Region of Iraq

The Kurdistan Region of Iraq (KRI), occupies the north and north-eastern portions of Iraq (Figure 1). KRI borders Iran to the East, Turkey to the North, Syria to the West, and the rest of Iraq to the South. Erbil is the capital of Kurdistan [18]. Erbil is the largest city in the Kurdistan region of Iraq, characterized by a mix of residential, commercial, and industrial zones. The city experiences a semi-arid climate, with hot summers and mild winters, which can influence pollutant dispersion and concentration.

2.2. Data Collection

The atmospheric data for this study were obtained from Arc GIS pro an advanced open-source platform developed through a partnership between Google and the National Aeronautics and Space Administration (NASA). Air pollutant data were primarily sourced from Sentinel-5P satellite sensors via Google Earth Engine (GEE). The study was conducted during the calendar year 2024. Monthly pollutant concentrations were derived from Sentinel-5P satellite datasets, covering January to December 2024. Complementary field sampling using calibrated portable instruments was conducted concurrently at five fixed locations. For validation and ground-level calibration, portable instruments were employed during fieldwork. These included the Aeroqual Series 500 for NO_2, O_3, and SO_2 (calibrated annually per ISO 9001 standards), the Testo 350 flue gas analyzer for CO and CH_4, and a UV Radiometer model UV-340 for UV measurements. Formaldehyde was measured using the PPM Technology Formalde meter htV-M. All devices were factory-calibrated and checked using certified calibration gases prior to deployment. Measurements were taken at 5 fixed urban/industrial sites within Erbil (specified in Appendix A), each sampled monthly over a 12-month period. The study targeted specific atmospheric gases: methane (CH_4), ozone (O_3), carbon monoxide (CO), nitrogen dioxide (NO_2), sulfur dioxide (SO_2), and methanal (CHOH).

Figure (1): Map demonstrate Erbil city Kurdistan-Iraq.

2.3. Index Calculation Methods

To evaluate air quality and related health risks, three indicators were calculated: Air Quality Index (AQI), WHO Health Risk Score, and Air Quality Health Index (AQHI).

2.3.1. Air Quality Index (AQI)

The AQI is widely used to represent the severity of air pollution and its potential health impact [14, 15, 19]. In this study, AQI values were calculated for CO, NO_2, and SO_2 using monthly average concentrations. Unlike the official U.S. EPA breakpoint-based formula, a simplified scaling method was applied due to data limitations. For each month, the highest pollutant-specific AQI value was taken as the overall air quality indicator. Table (1) shows the U.S. EPA categories for AQI ranges.

$$\mathbf{I} = \frac{(\mathbf{I\ Hi} - \mathbf{I\ Lo})}{(\mathbf{C\ Hi} - \mathbf{C\ Lo})} \mathbf{x}\ (\mathbf{C} - \mathbf{C\ Lo})\ + \mathbf{I\ Lo} \qquad (1)$$

where: I= AQI value, C = pollutant concentration (ppm), C_{Lo}, C_{Hi}= breakpoints in concentration I_{Lo}, I_{Hi} = corresponding AQI range (0–50, 51–100)

Table (1): Categories of Air Based on Air Quality Index (AQI) [14].

AQI Range	Air Quality Condition
0–50	Good
51–100	Moderate
101–150	Unhealthy for Sensitive Groups
151–200	Unhealthy
201–300	Very Unhealthy
>300	Hazardous

2.3.2. WHO Health Risk

Health risk was assessed by comparing measured pollutant concentrations with World Health Organization (WHO) guidelines [16, 17] (Table 2). A simple risk indicator was calculated as a ratio of the measured value to the WHO guideline value, expressed as a percentage:

$$\text{Risk } \% = \frac{\text{Measured Value}}{\text{WHO Limit}} \times 100 \qquad (2)$$

Table (2): WHO Guideline Values for Ambient Air Quality (WHO, 2021).

Pollutant	WHO Guideline
CO	≤9 ppm (8-hr)
NO_2	≤0.106 ppm (1-hr)
O_3	≤0.05 ppm
SO_2	≤0.015 ppm
HCHO	≤0.08 ppm
CH_4	No WHO limit
UV	Not applicable

2.3.3. Air Quality Health Index (AQHI)

The AQHI is designed to represent health risk from combined exposure to multiple pollutants [16, 17, 20, 21]. The AQHI was calculated as the mean of monthly concentrations of NO_2, and O_3. The relative contribution of each pollutant is shown by its β coefficient in Table (3).

$$\text{AQHI} = \frac{1000}{10.4} \times \left(e(0.000871 \times NO2 \times 1000) + e(0.000537 \times O3 \times 1000) - 2 \right) \qquad (3)$$

where: β O3=0.000871 and β NO2=0.000537.

Table (3): β Coefficients for AQHI Calculation.

Pollutant	β coefficient (per ppb)
NO_2	0.000537
O_3	0.000871
SO_2	0.000394
CO	2.96E-05

2.4. Comparison with Regulatory Standards

To put the observed concentrations into context, they were compared with Iraqi national standards and WHO guidelines. These reference limits are summarized in Table (4) [1, 16, 19, 21, 22].

Table (4): Iraqi Standards and WHO Guidelines for Ambient Air Quality.

Parameter	Averaging Period	Iraqi Standards	WHO Guidelines (µg/m³)
Carbon Monoxide	1-hour	35 ppm (40,250 µg/m³)	30,000
	8-hour	13 ppm (14,900 µg/m³)	10,000
Nitrogen Oxide (NO_2)	1-hour	0.1 ppm (188 µg/m³)	200
	Annual	0.05 ppm (94 µg/m³)	40
Sulphur Dioxide	1-hour	0.1 ppm (262 µg/m³)	500
	24-hour	0.04 ppm (105 µg/m³)	125 (Interim Target 1)
			50 (Guideline)

2.5. Statistical Analysis

The air quality data was analyzed using SPSS IBM Version 27 and GraphPad Prism 8.0 through a comprehensive statistical methodology. Initially, descriptive statistics summarized key metrics such as mean, median, standard deviation, Standard error and range of pollutant concentrations, provided insight into data distribution. Time series and trend analysis were conducted to identify significant temporal patterns, employing linear regression to quantify changes over time and seasonal decomposition to isolate recurring trends. Both linear and multiple regression analyses modeled relationships between pollutants and time, with statistical significance assessed via $p \leq 0.05$ and explanatory power evaluated through R-squared values. ANOVA was utilized for seasonal comparisons, while a correlation matrix explored interrelationships between pollutants.

3. Results

The study used data from Sentinel 5P satellite which was processed using Arc GIS and GEE programs. The analysis of air pollutant levels in Erbil showed temporal variations during the period of analysis. The data are organized systematically, beginning with pollutant categories, visual representations through figures and descriptive statistics, followed by risk assessments, indices, correlation analyses, principal component analysis, and seasonal decomposition.

3.1. Monthly Variability of Air Pollutants and UV Index

The monthly analysis revealed that the concentrations of air pollutants and ultraviolet (UV) radiation varied throughout the year (Figure 2). The recorded pollutants included carbon monoxide (CO), formaldehyde (HCHO), methane (CH_4), nitrogen dioxide (NO_2), ozone (O_3), sulfur dioxide (SO_2), and the UV index.

Carbon monoxide (CO) concentrations ranged from 5.90 ppm in October to 7.42 ppm in June, with an annual average of 6.66 ppm. These values remained below the WHO 8-hour exposure limit of 9 ppm (Table 1). Higher CO values in summer months may be attributed to increased combustion activities or photochemical reactions, while winter elevations possibly reflected emissions from heating systems.

Formaldehyde (HCHO) levels increased from 0.0139 ppm in January to a peak of 0.0382 ppm in July, then decreased to 0.0162 ppm in December, resulting in an annual mean of 0.0235 ppm. These concentrations surpassed the WHO recommended limit of 0.008 ppm in all months (Table 1), indicated consistent exposure above safety thresholds during the study period.

Methane (CH_4) values remained stable, ranged between 4.629 ppm in February and 4.701 ppm in June, with a mean of 4.6667 ppm. This consistency indicated background emissions with minor seasonal influence. The variation was minimal, supported by a standard deviation of 0.0223 ppm.

Nitrogen dioxide (NO_2) concentrations reached a maximum of 0.1004 ppm in June and a minimum of 0.0512 ppm in October, with an annual mean of 0.0674 ppm. These monthly values exceeded the WHO annual average limit of 0.021 ppm across all months, and the 1-hour standard of 0.106 ppm was approached in several months (Table 1), especially during warmer periods.

Ozone (O_3) concentrations remained consistently high, with the highest value of 0.3684 ppm in January and the lowest of 0.2997 ppm in September. The annual mean was 0.3314 ppm, which exceeded both the 8-hour limit (0.050 ppm) and the 1-hour exposure threshold (0.100 ppm) recommended by WHO (Table 1). These findings confirmed year-round ozone pollution of concern for public health.

Sulfur dioxide (SO_2) concentrations varied significantly, with the lowest value of 0.0019 ppm in June and the highest value of 0.0232 ppm in December. The mean annual concentration was 0.0076 ppm, which exceeded the WHO 24-hour guideline of 0.0075 ppm in several months (Figure 2), especially during colder months. However, all values remained below the WHO 10-minute limit of 0.175 ppm. The UV index showed strong seasonal dependence. It reached a peak value of 16.76 in January and dropped to 6.35 in June, with an annual average of 4.19 and a high standard deviation of 7.17. These variations were consistent with seasonal changes in solar radiation and atmospheric conditions.

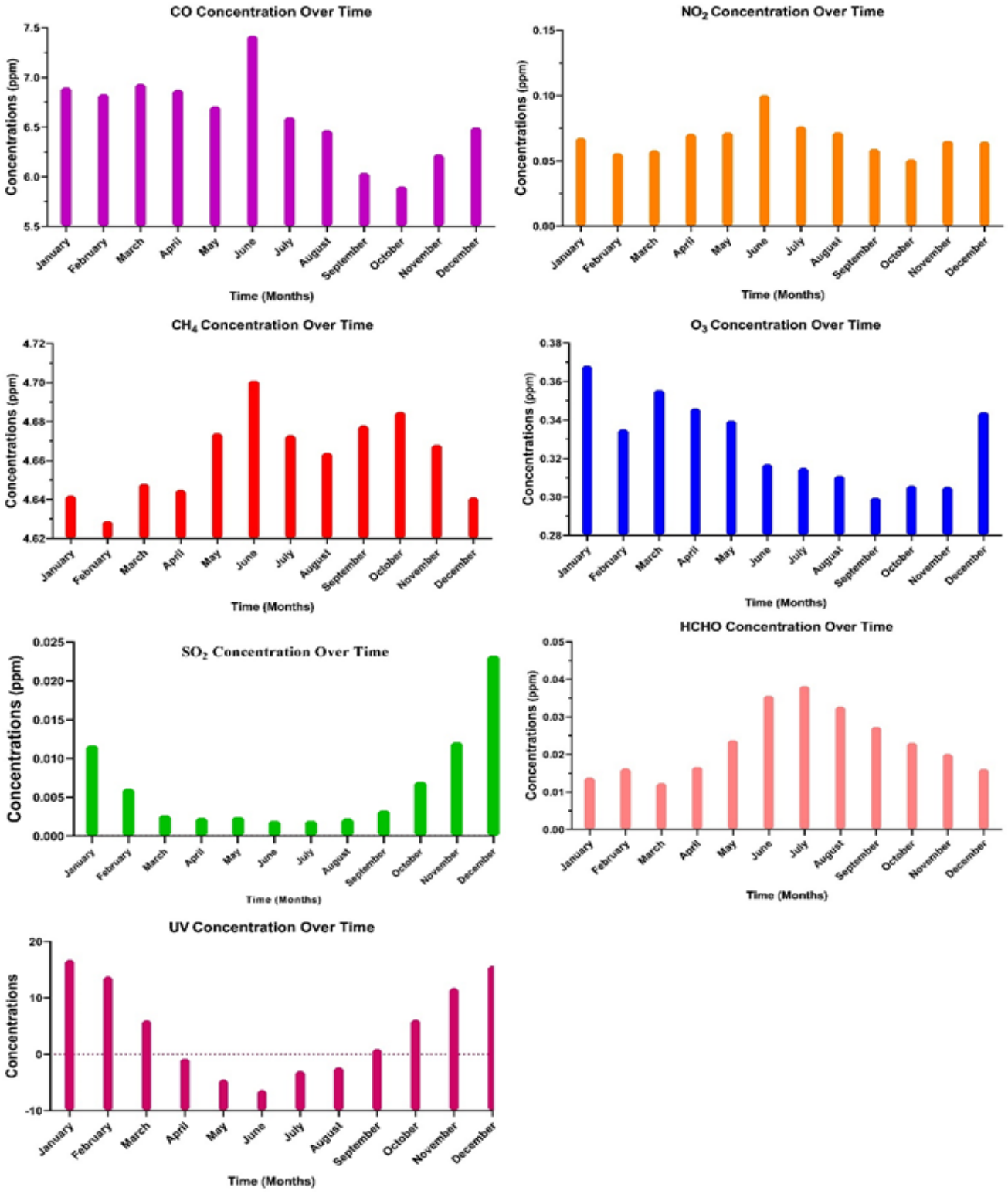

Figure (2): Time series plots for air pollutant concentrations over the 12 months.

3.2. Descriptive Statistics of Air Quality Parameters

Table (5) presented the descriptive statistics for all monitored pollutants and UV radiation over the 12-month study period. CO showed moderate variability (SD = 0.4218 ppm**,** CV = 6.33%**).** HCHO indicated a higher coefficient of variation (CV = 37.87%), revealed notable seasonal fluctuations. CH_4 was the most stable pollutant with a CV of 0.48%, whereas SO_2 demonstrated the highest variability (CV = 83.03%), likely due to

sporadic emissions associated with winter heating. The UV index showed the greatest fluctuation (CV = 171.24%**),** reflected greatest seasonal differences in atmospheric radiation exposure.

Table (5): Descriptive Statistics for Air Quality Data.

Pollutant	Min	Max	Mean	Std. Dev.	Std. Error	Iraqi Standards
CO (ppm)	5.9027	7.4196	6.6612	0.4218	0.1217	35 ppm (40,250 µg/m³)
HCHO (ppm)	0.0124	0.0382	0.0235	0.0089	0.0026	13 ppm (14,900 µg/m³)
CH_4 (ppm)	4.629	4.701	4.6667	0.0223	0.0064	0.1 ppm (188 µg/m³)
NO_2 (ppm)	0.0512	0.1004	0.0674	0.0138	0.004	0.05 ppm (94 µg/m³)
O_3 (ppm)	0.2997	0.3684	0.3314	0.0229	0.0066	0.1 ppm (262 µg/m³)
SO_2 (ppm)	0.0019	0.0232	0.0076	0.0065	0.0019	0.04 ppm (105 µg/m³)
UV	6.3533	16.7552	4.1916	7.168	2.0708	N/A

3.3. Linear Regression Trends

Linear regression analysis revealed declining trends for several pollutants, as detailed in Table (6). CO concentrations declined with a slope of -0.0405 (R^2 = 0.8243), while UV values decreased sharply (slope = -2.0886, R^2 = 0.8373). These trends were associated with the progression from summer to winter months. HCHO demonstrated an increasing trend (slope = 0.0010, R^2 = 0.6668), likely driven by temperature-dependent emissions. CH_4 also increased slowly over time (slope = 0.0503, R^2 = 0.6133). SO_2 showed a rising trend as well (slope = 0.0112, R^2 = 0.6499), particularly during colder months. O_3 showed a small downward trend (slope = -0.0006, R^2 = 0.5435), while NO_2 revealed no clear linear trend (slope = -0.0001, R^2 = 0.0284), indicated the influence of multiple short-term factors.

Table (6): Monthly Trend Analysis and Regression Modeling of Air Pollutants.

Pollutant	Slope (B)	Intercept	R^2 Value
CO	-0.0405	6.927	0.8243
HCHO	0.001	0.0138	0.6668
CH_4	0.0503	46.2697	0.6133
NO_2	-0.0001	0.0073	0.0284
O_3	-0.0006	0.0358	0.5435
SO_2	0.0112	0.0098	0.6499
UV	-2.0886	15.958	0.8373

3.4. Air Quality Index (AQI) and WHO Risk Assessment

The AQI values presented in Table (7), based on U.S. EPA standards, indicated persistent air quality concerns. O_3 values ranged from 391.0 to 465.07, with all months falling into the (Hazardous) or (Very Unhealthy) category. These high values indicated serious and prolonged public health risks. NO_2 reached an AQI of 259.51 in June, exceeding the 200 AQI threshold during several months and indicating "Very Unhealthy" conditions. SO_2 values remained low during summer but increased significantly and reached 170.13 in December, exceeding the (Unhealthy for Sensitive Groups) range. CO values remained in the (Moderate) range throughout the year, peaked in June (80.20) and reaching a low in October (65.03).

Table (7): Monthly Air Quality Index (AQI) Values for CO, NO_2, SO_2 and O_3.

Month	AQI (CO)	AQI (NO_2)	AQI (SO_2)	AQI O_3
January	75	205.08	119.43	465.07
February	74.31	184.59	82.47	432.53
March	75.34	188.37	38.18	452.54
April	74.75	210.56	33	443.24
May	73.08	212.3	35.14	436.89

June	80.2	259.51	27.63	414.76
July	71.98	219.69	28.16	412.9
August	70.7	212.66	31.94	408.93
September	66.4	190.37	46.88	397.78
October	65.03	176.73	93.71	403.79
November	68.25	201.71	121.05	403.25
December	70.97	199.53	170.13	441.33

Table (8) presented monthly health risk percentages for each pollutant compared to WHO guideline values (Table 1). O_3 posed the highest threat, contributing 20.6% to 25.3% of the maximum safe exposure level. These values confirmed continuous exposure beyond recommended safety limits. NO_2 health risk values reached 19.3% in June and remained above 15% in several other months, indicated chronic exposure. CO risk percentages were lower, between 7.0% and 8.8%, while SO_2 posed a notable risk in winter (5.0% in December) but remained low in other months.

Table (8): Monthly WHO Risk Percentages for Pollutants.

Month	CO Risk %	NO_2 Risk %	SO_2 Risk %	O_3 Risk %
January	8.2	13	2.5	25.3
February	8.1	10.7	1.3	23
March	8.3	11.1	0.6	24.4
April	8.2	13.6	0.5	23.7
May	8	13.8	0.5	23.3
June	8.8	19.3	0.4	21.8
July	7.9	14.7	0.4	21.6
August	7.7	13.9	0.5	21.4
September	7.2	11.4	0.7	20.6
October	7	9.9	1.5	21
November	7.4	12.6	2.6	20.9
December	7.7	12.5	5	23.6

3.5. Correlation and Regression Analysis

The correlation matrix in Table (9) revealed several strong positive associations among the measured pollutants. CO recorded significant positive correlations with HCHO ($r = 0.687$) and NO_2 ($r = 0.681$). HCHO and CH_4 were strongly correlated ($r = 0.802$), revealed similar emission sources or formation pathways. UV levels correlated positively with SO_2 ($r = 0.765$), but negatively with HCHO ($r = -0.742$), CH_4 ($r = -0.627$), and NO_2 ($r = -0.572$). These negative relationships indicated the role of these pollutants in absorbing solar radiation or participating in photochemical reactions that reduce UV intensity.

Table (9): Correlation Matrix for Pollutants.

Pollutant	CO	HCHO	CH_4	NO_2	O_3	SO_2	UV
CO	1	0.687	0.142	0.681	0.634	-0.101	-0.068
HCHO	0.687	1	0.802	0.651	-0.55	-0.451	-0.742
CH_4	0.142	0.802	1	0.411	-0.58	-0.365	-0.627
NO_2	0.681	0.651	0.411	1	-0.46	-0.07	-0.572
O_3	0.634	-0.55	-0.58	-0.46	1	0.29	0.163
SO_2	-0.101	-0.451	-0.365	-0.07	0.29	1	0.765
UV	-0.068	-0.742	-0.627	-0.572	0.163	0.765	1

3.6. Principal Component Analysis and Pollutant Standards Index

The Principal Component Analysis (PCA) results, as presented in Table (10), revealed three principal components that together explained the majority of the variability of the dataset. The first component,

accounting for 48.1% of the variance, was primarily associated with CO, NO_2, and HCHO. The second component, explaining 20.4% of the variance, was dominated by SO_2 and UV radiation. The third component, contributing 12.4% of the variance, was linked to CH_4 and O_3. Collectively, these three components explained 80.9% of the total variance, providing a robust basis for interpreting common pollution sources and seasonal trends

Table (10): Total Variance Explained by Principal Components Analysis (PCA).

Component	Eigenvalue	% of Variance	Cumulative %
1	3.37	48.1	48.1
2	1.43	20.4	68.5
3	0.87	12.4	80.9
4	0.52	7.4	88.3
5	0.4	5.7	94
6	0.28	4	98
7	0.13	1.7	100

3.7. Air Quality Health Index (AQHI) Pattern

The monthly Air Quality Health Index (AQHI) values indicated noticeable seasonal variability throughout the year. As presented in Figure (3), AQHI values ranged from a minimum of 6.31 in October to a maximum of 10.02 in June, reflected changes in pollutant concentrations and meteorological conditions. During the winter months, AQHI values remained relatively high, with January and December reported 8.4 and 8.5, respectively. This trend was likely influenced by increased combustion activities for heating and atmospheric stability, which limited pollutant dispersion. Similarly, November registered a value of 7.56, maintaining the higher AQHI pattern observed in cooler months.

In contrast, the summer months showed slightly higher fluctuations. The index peaked in June at 10.02, the highest value observed during the study period, likely due to elevated photochemical activity leading to ozone formation, combined with enhanced solar radiation and reduced wind speeds. July and August recorded AQHI values of 8.0 and 7.64, respectively, which were still within the higher-risk category according to health-based standards. The lowest AQHI values occurred in early autumn, with October recorded 6.31 and September 6.62, suggesting improved dispersion conditions and lower precursor emissions during this period. Spring months showed moderate AQHI levels, with April and May recorded 7.94 and 7.95, respectively (Figure 4).

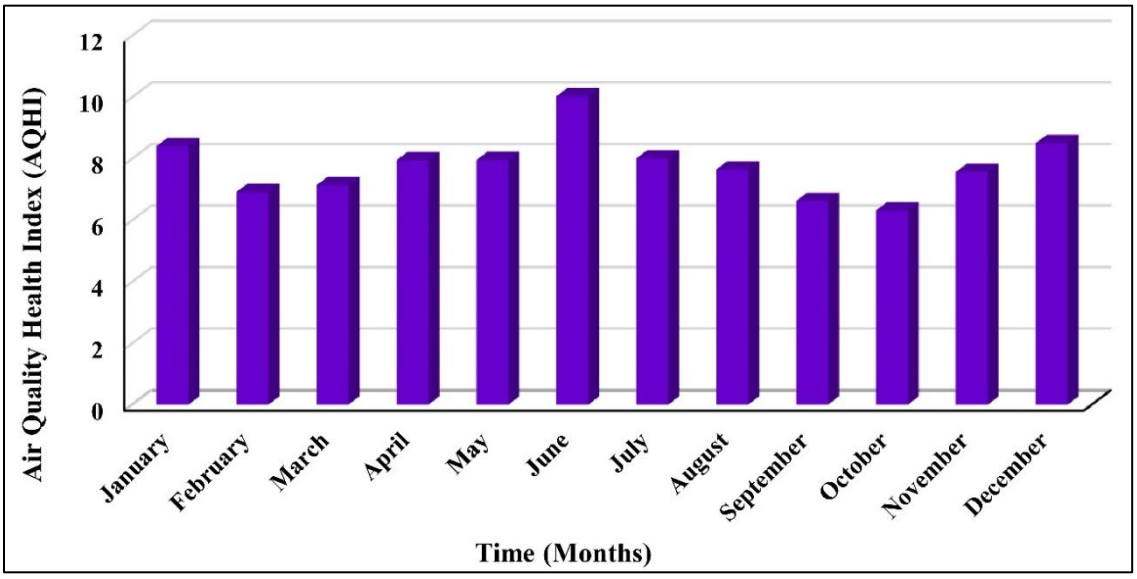

Figure (3): Monthly Air Quality Hazard Index (AQHI) Trends

3.8. Spatial Distribution of Air Pollutants in Erbil

The highest levels of air pollutants were significantly observed in the central areas of Erbil and several surrounding regions, as shown in Figure (4). The overall spatial distribution of air pollutants in Erbil over the 12-month period, illustrated in these maps, indicated that the highest concentrations of NO_2 occurred in the central and northern parts of the city, exceeding 0.0004 mol/m². These areas, likely characterized by heavy traffic and industrial activity, revealed the most significant NO_2 pollution, whereas peripheral regions showed lower concentrations. Elevated SO_2 levels were predominantly found in the southern and southwestern regions, reached concentrations of up to 0.0005 mol/m². The central parts of Erbil experienced the highest O_3 concentrations, measuring 0.125 mol/m². This distribution pattern indicated photochemical smog formation resulting from vehicular and industrial emissions combined with strong sunlight. CH_4 concentrations were highest in the northern and western regions, exceeding 1935 mol/m², indicated substantial methane sources possibly related to waste management or agricultural activities. The greatest CO concentrations were recorded in the central and eastern parts of the city, with values up to 0.030 mol/m², consistent with areas of dense traffic and industrial zones. The UV radiation index peaked in the western and central regions, reached 0.685 mol/m², this pattern may be influenced by local topography and atmospheric conditions that permit higher UV penetration. Lastly, the highest concentrations of formaldehyde (HCHO) were observed in central Erbil, with values reached 0.00016 mol/m², likely linked to vehicular emissions, heavy traffic, and industrial sources.

4. Discussion

The results demonstrated significant seasonal variations in pollutant concentrations in Erbil, consistent with global urban air quality patterns. Concentrations of CO, NO_2, and SO_2 were highest during the winter months, while O_3 levels peaked from late winter to early spring. These trends align with observations reported in Chengdu, China, and Curitiba, Brazil, where CO and SO_2 concentrations reached their maximum in winter and minimum in summer, whereas O_3 showed an inverse seasonal cycle [23, 24]. CO and NO_2 levels in Erbil peaked in colder months, similar with the findings in Chinese megacities where winter emissions from traffic and industry, combined with low boundary layer heights, led to elevated winter concentrations [23, 25]. The study observations demonstrated that the CO concentrations peaked in December and January, while NO_2 reached its annual maximum in June but remained elevated throughout the winter months, indicated its association with combustion sources and limited atmospheric dispersion. O_3 levels in Erbil were highest in January, declined during the summer, and increased again in autumn. This pattern corresponds to the winter to early spring ozone peaks observed in Dhaka, Bangladesh, where volatile organic compound (VOC) emissions and photochemical activity under clear skies produced similar seasonal trends [26, 27]. Comparable seasonal ozone cycles were documented in Malaysia's northeast monsoon period [28]. Similar trends were reported in a recent study from Kirkuk by Husain (2024) [29] and Saleh (2024) [30], were reported that NO_2 and CO levels surged in winter due to heating demands. In Mosul, SO_2 concentrations were also observed to exceed WHO limits in December, consistent with our findings for Erbil [31, 32].

A strong negative correlation was observed between UV and primary pollutants (HCHO, CH_4, NO_2), indicated active photochemical processing. Similar inverse relationships between summer O_3 and NO_x were reported in urban India and Sri Lanka, attributed to NO_2 photolysis [26, 33]. Regression analysis revealed elevated levels of HCHO and CH_4 during the warmer months, indicative of enhanced secondary pollutant formation. HCHO concentrations peaked in July and exceeded the WHO guideline values, in agreement with summer maxima reported in both remote sensing and in-situ studies. These elevated concentrations were attributed to the oxidation of biogenic volatile organic compounds (VOCs) and intensified photochemical activity [23, 26]. CH_4 revealed minimal seasonal variation, consistent with evidence that methane levels are largely influenced by regional background sources rather than local seasonal factors [28]. SO_2 concentrations increased during the winter months, with a clear peak in December. This trend is consistent with findings from Poland and other European regions, where increased use of heating and stable atmospheric conditions during winter lead to higher levels of SO_2 pollution [23, 33]. This winter peak corresponded to both AQI and WHO risk increases during the cold months.

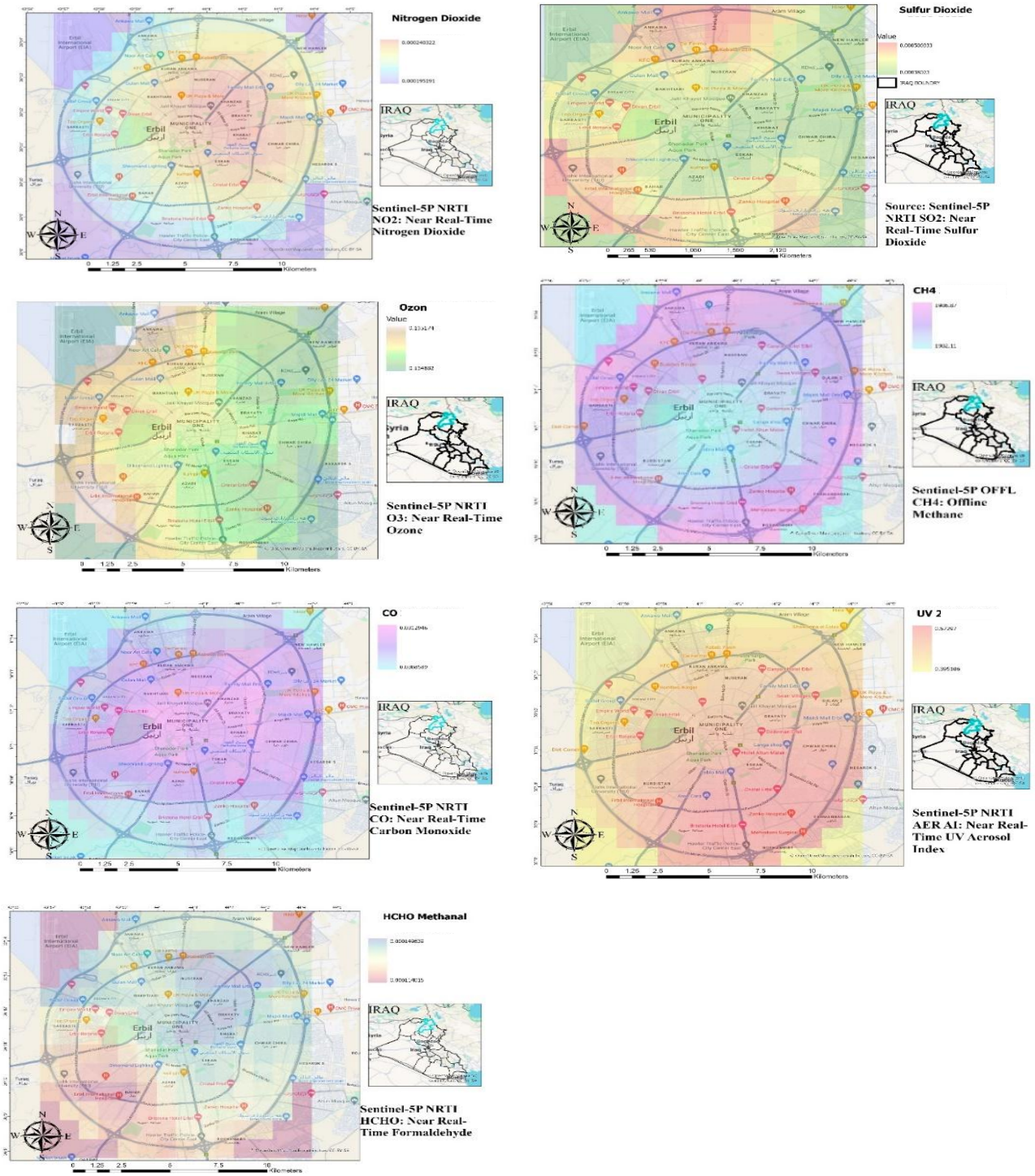

Figure (4): spatial distribution of air pollutants in Erbil-Kurdistan region of Iraq.

5. Conclusion

This study provided a comprehensive evaluation of the seasonal and spatial variations of major air pollutants across Erbil over a complete annual cycle. The results demonstrated that concentrations of carbon monoxide (CO), nitrogen dioxide (NO_2), sulfur dioxide (SO_2), and methane (CH_4) were highest during the winter months, reflecting increased combustion-related activities and atmospheric conditions that restricted pollutant dispersion. In contrast, levels of ozone (O_3) and formaldehyde (HCHO) peaked during the warmer months, driven by enhanced photochemical reactions under elevated solar radiation, as evidenced by seasonal fluctuations in the ultraviolet (UV) index. Methane concentrations remained relatively stable throughout the year, suggesting

dominant contributions from consistent background sources. Regression and correlation analyses identified CO and NO_2 as key contributors to air quality degradation. Principal Component Analysis (PCA) effectively clustered pollutants based on shared sources and seasonal dynamics. Air Quality Index (AQI) assessments frequently exceeded the World Health Organization (WHO) guideline thresholds, particularly for O_3 and NO_2, indicated persistent public health risks. To address these concerns, the study recommended the implementation of stricter emission controls targeting vehicular and industrial sources, especially during winter when pollutant concentrations were most severe. Additional mitigation strategies included the expansion of air quality monitoring networks, increased public awareness campaigns, the promotion of cleaner fuel alternatives, and the enhancement of urban green infrastructure to reduce pollutant accumulation. Future research was recommended to broaden spatial coverage and investigate the influence of meteorological parameters on pollutant dispersion, thereby supporting evidence-based environmental policy development

Conflict of Interest: The authors declare that there are no conflicts of interest associated with this research project. We have no financial or personal relationships that could potentially bias our work or influence the interpretation of the results.

References

[1] A. A. Almetwally, M. Bin-Jumah, and A. A. Allam, "Ambient air pollution and its influence on human health and welfare: an overview," *Environmental Science and Pollution Research*, vol. 27, pp. 24815-24830. https://doi.org/10.1007/s11356-020-08362-4 2020.

[2] S. J. Mohammed, S. M. Ahmed, M. Q. Qadr, H. Blbas, A. N. Ali, and A. F. Saber, "Climate Change Anxiety Symptoms in the Kurdistan Region of Iraq," *Journal of Pioneering Medical Sciences*, vol. 14, pp. 23-30. https://doi.org/10.47310/jpms2025140215, 2025.

[3] I. Manisalidis, E. Stavropoulou, A. Stavropoulos, and E. Bezirtzoglou, "Environmental and health impacts of air pollution: a review," *Frontiers in public health*, vol. 8, p. 14. https://doi.org/10.3389/fpubh.2020.00014 2020.

[4] V. Singh, R. Srivastava, and A. K. Bhatt, "Major Air Pollutants," in *Battling Air and Water Pollution: Protecting Our Planet's Vital Resources*: Springer, 2025, pp. 31-42. https://doi.org/10.1007/978-981-96-4375-2_3.

[5] S. M. Awadh, "Impact of North African sand and dust storms on the Middle East using Iraq as an example: Causes, sources, and mitigation," *Atmosphere*, vol. 14, no. 1, p. 180. https://doi.org/10.3390/atmos14010180, 2023.

[6] A. A. Attiya, "Assessment of dust events above Iraq using remote sensing of the atmosphere and Arc GIS techniques," University of Wollongong, 2020.

[7] R. Munsif, M. Zubair, A. Aziz, and M. N. Zafar, "Industrial air emission pollution: potential sources and sustainable mitigation," in *Environmental emissions*: IntechOpen, 2021.

[8] S. M. Nasir, K. V. Kamran, T. Blaschke, and S. Karimzadeh, "Change of land use/land cover in kurdistan region of Iraq: A semi-automated object-based approach," *Remote Sensing Applications: Society and Environment*, vol. 26, p. 100713. https://doi.org/10.1016/j.rsase.2022.100713, 2022.

[9] A. A. Al-Salman and R. M. TaghiEbadi, "Mitigation Strategies for Reducing of Air Pollutant, Case Study: Al-Hilla City-Babylon Province/Iraq," *Annals of the Romanian Society for Cell Biology*, pp. 7460–7469-7460–7469, 2021.

[10] M. T. Chaichan, H. A. Kazem, and T. A. Abed, "Traffic and outdoor air pollution levels near highways in Baghdad, Iraq," *Environment, development and sustainability*, vol. 20, pp. 589-603. DOI: 10.1007/s10668-016-9900-x, 2018.

[11] A. Al-Fouadi and D. Parkin, "Cancer in Iraq: seven years' data from the Baghdad Tumour Registry," *International journal of cancer*, vol. 34, no. 2, pp. 207-213. https://doi.org/10.1002/ijc.2910340211, 1984.

[12] M. Karwan *et al.*, "Cancer incidence in the Kurdistan region of Iraq: Results of a seven-year cancer registration in Erbil and Duhok Governorates," *Asian Pacific Journal of Cancer Prevention: APJCP*, vol. 23, no. 2, p. 601. https://doi.org/10.31557/APJCP.2022.23.2.601, 2022.

[13] A. M. Hussain and R. K. Lafta, "Cancer trends in Iraq 2000–2016," *Oman medical journal*, vol. 36, no. 1, p. e219. https://doi.org/10.5001/omj.2021.18, 2021.

[14] A. Q. Index, "A guide to air quality and your health," *USA: EPA*, 2009.

[15] C. A. Act, R. Act, and R. Act, "Environmental protection agency (EPA)," *Report on Carcinogens*, vol. 168, 2006.
[16] WHO, "WHO global air quality guidelines," ed: World Health Organization Geneva, Switzerland, 2021.
[17] A. Goshua, C. A. Akdis, and K. C. Nadeau, "World Health Organization global air quality guideline recommendations: executive summary," *Allergy*, vol. 77, no. 7, pp. 1955-1960, 2022.
[18] S. M. Shareef, "Electronic government adoption based on citizen-centric approach in regional government in developing countries: the case of Kurdistan Region of Iraq (KRI)," University of East London, 2012.
[19] L. Veal, "United States environmental protection agency," *US Environmental Protection Agency (EPA)(2005) National Management Measures to Control Non-Point Source Pollution for Urban Areas*, 2021.
[20] D. M. Stieb, R. T. Burnett, M. Smith-Doiron, O. Brion, H. H. Shin, and V. Economou, "A new multipollutant, no-threshold air quality health index based on short-term associations observed in daily time-series analyses," *Journal of the Air & Waste Management Association*, vol. 58, no. 3, pp. 435-450, 2008.
[21] Y. Nazarenko, D. Pal, and P. A. Ariya, "Air quality standards for the concentration of particulate matter 2.5, global descriptive analysis," *Bulletin of the World Health Organization*, vol. 99, no. 2, p. 125, 2020.
[22] S. Faridi *et al.*, "Ambient air quality standards and policies in eastern mediterranean countries: a review," *International Journal of Public Health*, vol. 68, p. 1605352. https://doi.org/10.3389/ijph.2023.1605352, 2023.
[23] K. Xiao, Y. Wang, G. Wu, B. Fu, and Y. Zhu, "Spatiotemporal characteristics of air pollutants (PM10, PM2. 5, SO2, NO2, O3, and CO) in the inland basin city of Chengdu, southwest China," *Atmosphere*, vol. 9, no. 2, p. 74. https://doi.org/10.3390/atmos9020074, 2018.
[24] V. Fioletov, C. A. McLinden, D. Griffin, X. Zhao, and H. Eskes, "Global seasonal urban, industrial, and background NO2 estimated from TROPOMI satellite observations," *Atmospheric Chemistry and Physics*, vol. 25, no. 1, pp. 575-596. https://doi.org/10.5194/acp-25-575-2025, 2025.
[25] P. Krecl, L. B. Castro, A. C. Targino, and G. Y. Oukawa, "Spatio-temporal variability and trends of air pollutants in the Metropolitan Area of Curitiba," *Heliyon*, vol. 10, no. 23, p. https://doi.org/10.1016/j.heliyon.2024.e40651, 2024.
[26] S. R. Morshed *et al.*, "Decoding seasonal variability of air pollutants with climate factors: A geostatistical approach using multimodal regression models for informed climate change mitigation," *Environmental Pollution*, vol. 345, p. 123463. https://doi.org/10.1016/j.envpol.2024.123463, 2024.
[27] A. Rahman and N. R. Nasher, "Forecasting hourly ozone concentration using functional time series model—A case study in the coastal area of bangladesh," *Environmental Modeling & Assessment*, vol. 29, no. 1, pp. 125-134. https://doi.org/10.1007/s10666-023-09928-8, 2024.
[28] P. Lalitaporn, G. Kurata, Y. Matsuoka, N. Thongboonchoo, and V. Surapipith, "Long-term analysis of NO2, CO, and AOD seasonal variability using satellite observations over Asia and intercomparison with emission inventories and model," *Air Quality, Atmosphere & Health*, vol. 6, no. 4, pp. 655-672. https://doi.org/10.1007/s11869-013-0205-z, 2013.
[29] M. M. Husain, "An Experimental Study on Electricity Generator Emissions and Their Environmental Impact in Kirkuk City," *Advances in Mechanical and Materials Engineering*, vol. 41, no. 1, pp. 113-123. https://doi.org/10.7862/rm.2024.11, 2024.
[30] S. H. Saleh, "Assessment of Air Pollutants for Baba Industrial Area at Kirkuk Oil Field, Iraq," *The Iraqi Geological Journal*, pp. 125-137. https://doi.org/10.46717/igj.57.2E.10ms-2024-11-19, 2024.
[31] N. M. Abbas and J. M. Rajab, "Sulfur Dioxide (SO2) anthropogenic emissions distributions over Iraq (2000-2009) using MERRA-2 data," *Al-Mustansiriyah Journal of Science*, vol. 33, no. 4, pp. 27-33. https://doi.org/10.23851/mjs.v33i4.1187, 2022.
[32] Z. Altahaan and D. Dobslaw, "Assessing Long-Term Post-Conflict Air Pollution: Trends and Implications for Air Quality in Mosul, Iraq," *Atmosphere*, vol. 16, no. 7, p. 756. https://doi.org/10.3390/atmos16070756, 2025.
[33] X. Li *et al.*, "Variation characteristics and coordinated emission reduction of air pollutants in megacity of Chengdu-Chongqing economic circle under dual carbon goal," *Environmental Engineering Research*, vol. 29, no. 4, p. https://doi.org/10.4491/eer.2023.475, 2024.